Progress in Propulsion Physics **2** (2011) 35-58

HETEROGENEOUS PROPELLANT INTERNAL BALLISTICS: CRITICISM AND REGENERATION

R. L. Glick

Stone Engineering Division
Analytical Services, Inc.
Huntsville, AL, USA

Although heterogeneous propellant and its innately nondeterministic, chemically discrete morphology dominates applications, ballistic-characterization deterministic time-mean burning rate and acoustic admittance measures' absence of explicit, nondeterministic information requires homogeneous propellant with a smooth, uniformly regressing burning surface: inadequate boundary conditions for heterogeneous propellant grained applications. The past age overcame this dichotomy with one-dimensional (1D) models and empirical knowledge from numerous, adequately supported motor developments and supplementary experiments. However, current cost and risk constraints inhibit this approach. Moreover, its fundamental science approach is more sensitive to incomplete boundary condition information (garbage-in still equals garbage-out) and more is expected. This work critiques this situation and sketches a path forward based on enhanced ballistic and motor characterizations in the workplace and approximate model and apparatus developments mentored by CSAR DNS capabilities (or equivalent).

NOMENCLATURE

a	acoustic speed
A	area
$\mathcal{A}_b$	pressure coupled acoustic admittance, $(\widehat{u}_b/\overline{a}_f)/(\widehat{p}_E/\overline{p}_E)$
c	specific heat
C^*	characteristic velocity
$\mathcal{F}\{\}_{\omega_c}^{(\gamma)}$	real part of Fourier transform at circular frequency ω_c
g	acceleration
L^*	characteristic chamber length, V/A_t
$\mathcal{M}$	molecular weight
p	pressure

Article available at http://www.eucass-proceedings.eu or http://dx.doi.org/10.1051/eucass/201102035

r_b	burning rate
R_p	universal gas constant
$\mathcal{R}_p$	pressure-coupled mass response function, $(\widehat{r}_b/\overline{r}_b)(\widehat{p}_E/\overline{p}_E)$
t	time
t_B	burn time
T	temperature
$\vec{u}$	velocity vector
web	web for burning rate characterization
$\vec{x}$	position vector
α	thermal diffusivity
γ	specific heat ratio
ε	nondimensional pressure ratio, $\widehat{p}/\overline{p}$
$\overleftrightarrow{\tau}$	shear stress tensor
τ_{ch}	chamber residence time, $\gamma L^* C^*/a_f^2$
Θ_f	pressure-coupled flame temperature response function, $(\widehat{T}_f/\overline{T}_f)/(\widehat{p}/\overline{p})$
Ψ	rotating valve throat area function
ω_c	circular frequency

Subscripts

b	planar projection
E	environmental value
f	flame state
g	gas phase
p	propellant
s	burning surface
t	throat
1,2	states 1 and 2

Special

b'	fluctuating part of b
$\overline{b}$	time-mean part of b
$\widehat{b}$	amplitude of b

Abbreviations

1D	one-dimensional
Al	aluminum
AP	ammonium perchlorate
BC	boundary condition

BS	burning surface
CESE	conservation element and solution element
CFD	computational fluid dynamics
CSAR	Center for Simulation of Advanced Rockets, University of Illinois at Urbana/Champaign
DNS	direct numerical simulation
HOD	homogeneous one-dimensional
HTPB	hydroxyl-terminated polybutadiene
MHD	magnetohydrodynamic
QS	quasi-steady
RS	reduced smoke

1 INTRODUCTION

Solid propellant applications are dominated by heterogeneous propellants [1, 2] and their innately nondeterministic (well mixed), polydisperse, chemically discrete at-the-oxidizer-particles-scale morphology, e. g., Fig. 1 and Figs. 1–4 in [3] cut surface, deflagration, snapshot Schlieren, and burning surface topography images, and [4] tomograms*. Moreover, this domination is expected to continue [6]. In contrast, internal ballistics have always been ruled by ballistic characterization [7–9] deterministic time-mean burning rate

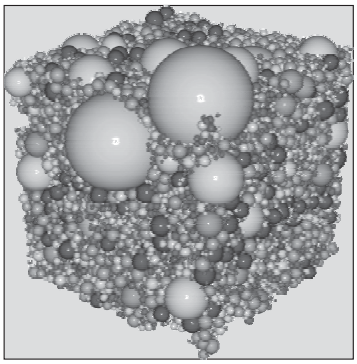

Figure 1 Propellant packing (courtesy T. A. Jackson/CSAR)

$$\overline{r}_b(\overline{p}, T_0) \equiv \frac{\text{web}}{t_B} \tag{1}$$

and pressure coupled acoustic admittance

$$\mathcal{A}_b \equiv \frac{\widehat{u}_b/\overline{a}_f}{\widehat{p}_E/\overline{p}_E} \tag{2}$$

measures. Therefore, because the instantaneous mass efflux from a small area of a heterogeneous propellant BS in a quiescent environment is

$$\iint\limits_{\Delta A_s} \rho_{s,c}(\vec{x},t) r_s(\vec{x},t)\, dA_s = \overline{r}_b \rho_p \Delta A_b \,,$$

the absence of explicit $\rho_{s,c}(\vec{x},t)$, $r_s(\vec{x},t)$, etc. and BS topography information requires the implicit assumption of a smooth, planar, chemically homogeneous,

*If possible, readers should have these images in view as they read this text.

and uniformly regressing BS for internal ballistic predictions based on the measures of Eqs. (1) and (2). Consequently, information deficiencies in ballistic characterization invisibly replace heterogeneous-propellant grain of an application with idealized homogeneous propellant for performance predictions (what is the alternative?).

Although fundamental field equations that govern flow field, e. g., Navier–Stokes equations

$$\frac{\rho D\vec{u}}{Dt} = -\nabla p - \nabla \overleftrightarrow{\tau} + \rho\vec{g} \tag{3}$$

and condensed phase apply to either deterministic or nondeterministic BCs, the absence of explicit $\rho_{s,c}(\vec{x},t)$, $r_s(\vec{x},t)$, etc. and BS topography information in ballistic characterization precludes robust flow field predictions and deep understanding of the phenomena, e.g., physical phenomena of [3], Figs. 3 and 4 cannot be predicted. Moreover, because cold flow analogs cannot mimic heterogeneous propellants $\vec{u}_{s,g}(\vec{x},t)$, $T_{s,g}(\vec{x},t)$, $\mathcal{M}_{s,g}(\vec{x},t)$, and BS topography BCs, these experiments cannot robustly mimic heterogeneous propellant deflagration sourced flow fields. Consequently, attempts to idealize cold flow analog experiments without perspective to heterogeneous propellants' innate challenges [10] suggest their purpose is to validate idealized flow field models rather than to understand application phenomena.

Deviations from heterogeneous propellant reality created by the idealized BCs in ballistic characterization are instructive because they illustrate physical consequences associated with inadequate ballistic characterization. Summerfield *et al.* [3] provided Schlieren image density variations across the BS extend to an altitude of roughly 3 mm (the strand approximate width) (Fig. 3). Therefore, Eq. (3) predicting a pressure gradient across the BS will create relative motions among its constituents of different density thereby altering mixing and chemical energy deposition*, i. e., phenomena akin to King's [12] flame-bending erosive burning model — but different. Consequently, heterogeneous propellant provides physical mechanisms for erosive burning, velocity coupling, acceleration augmentation, etc. absent at idealized homogeneous propellant BCs.

Acoustic stability theory [13]† assumes that the rate of specific flow work at the inflow surface due to sinusoidal pressure oscillations of amplitude $\widehat{p}_E$ and circular frequency ω in the environment is

$$R_u\mathcal{F}\left\{\oint_{\Delta A_s}\frac{\rho_{s,c}(\vec{x},t)r_s(\vec{x},t)T_{s,g}(\vec{x},t)}{\mathcal{M}_{s,g}(\vec{x},t)}\,\frac{dA_s}{\Delta A_b}\right\}^{(r)}_{\omega_c} \stackrel{?}{=} \frac{\overline{a}_f}{\overline{p}_E}\left\{\widehat{p}_E^{\,2}\mathcal{A}_b^{(r)}\right\}_{\omega_c} \tag{4}$$

*Povinelli's [11] CN spectra *for another formulation at low pressure* suggests that chemical energy deposition occurs to altitudes of ~ 3 mm.

†Reference [13] includes a brief review of acoustic and hydrodynamic stability work and future activities.

when the BS efflux is an ideal gas. Because the right hand side's quiescent environment BS efflux is truly steady state, environmental pressure oscillations, e. g., $\widehat{p}_E > 0$, are necessary and create acoustic energy at its frequency. However, since the left hand side's deflagration in a quiescent environment is typically nonsteady at the oxidizer particles scales and correlated by the deflagration wave propagation through the propellant morphology, its deflagration can create broadband acoustic energy when $\widehat{p}_E = 0$. Therefore,

(a) heterogeneous propellant deflagration in a quiescent environment typically creates broadband acoustic energy (listen to a burning strand);

(b) stable (sustained exponential growths do not occur), heterogeneous propellant grained applications typically exhibit anomalous, low amplitude, omni-present pressure oscillations over a broad bandwidth (measure them); and

(c) since steady inflow through a porous wall, e. g., $\vec{u}_{s,g} = \vec{u}_{s,g}(\vec{x})$, cannot produce acoustic energy per Eq. (4), omni-present pressure oscillations in cold flow analogs cannot arise from this mechanism, e. g., cold flow analogs cannot robustly mimic heterogeneous propellant deflagration sourced flows.

Item (b) infers flow field stability models that assume $\vec{u}\,'(\vec{x},t) = p'(\vec{x},t) = 0$ for their stable state are not robust for heterogeneous propellant grained applications and preclude deep understanding, i. e., item (b) phenomena must be attributed to another source. Item (b) also infers CFD simulations must be fluid dynamically and acoustically robust *concurrently* if predictions are to provide deep understanding. Because the CESE method alone meets this criterion (I-Shih Chang, personnal discussion, 2006), CFD results from other numerical methods may not be robust for heterogeneous propellant grained applications.

Van Moorhem [14] spatially averaged fundamental flow field equations to one spatial dimension for ports whose scalar flow area is independent of time (a typical acoustic stability theory assumption). Although valid for deterministic, idealized homogeneous propellants, it is not for heterogeneous propellant nondeterministic variations of the flow area perimeter geometry *at the oxidizer particles scales* (see the BS images of [3], Fig. 4) because it eliminates items (a) and (b) phenomena. Mathematically, this presumption eliminates nondeterministic perimeter motions (at fixed scalar port area) that correlate with variables averaged with Liebnitz rule. Thus, on the one hand, naive spatial dimension reductions can subtly corrupt apparently robust mathematical developments when heterogeneous propellant is involved.

On the other hand, the deflagration wave can ameliorate the virgin propellant heterogeneity near the BS, e. g., Kubota's [15] polyurethane, RDX propellant effectively homogeneous BS composition and deflagration processes. Therefore, heterogeneous propellant deflagration processes can range from those that mimic

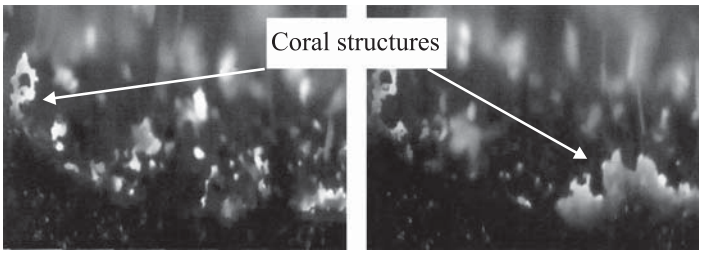

Figure 2 The HTPB/AP/nanoAl propellant deflagration at pressure $\sim$ 72 psi [5] (courtesy F. Maggi, Politecnico di Milano)

idealized homogeneous propellant BCs to those whose $\rho_{s,c}(\vec{x}_s, t)$, $r_s(\vec{x}_s, t)$, etc. and BS topography deviates significantly from this idealization. However, because Eq. (1) burning rates for these formulations can be effectively identical, $\overline{r}_b(p, T_0)$ information *per se* cannot robustly discriminate between those that mimic idealized homogeneous propellant and those do not, i. e., classical Crawford strand burner $\overline{r}_b(p, T_0)$ data are impotent for this purpose.

Figure 2 illustrates deflagration phenomena for an HTPB/AP/$\sim$ 3% nanoAl propellant. The coral structure in the left image suggests characteristics of an Al skeleton layer [16]. However, the coral structure in the right image and elsewhere in the images is solid *suggesting* hydrogen producing nanoAl + HTPB reactions (NEWPEP Code) have created intuminescent binder that extruded around the coarser AP particles (suggested by the cine images) to form these structures. Moreover, additional experiments demonstrate that burning rate and its pressure and temperature sensitivities for these formulations are effectively independent of nanoAl content when *it is small* (David Booth, personal discussion, summer 2007). Therefore, for these iso-$\overline{r}_b(p, T_0)$ propellants, nanoAl enables significant BS *topography* variations at fixed burning rate and effectively fixed chemical composition — phenomena impossible for idealized homogeneous propellants smooth BS* presumption. Consequently, heterogeneity presents an additional degree of freedom for propellant formulation that can be employed to optimize the propellant for an application.

For example, the maximum amplitude of RS Maverick's omni-present pressure oscillations were reduced by a factor of $\sim$ 50 for iso-$\overline{r}_b(p, T_0)$ (chemical composition altered $< 3\%$) constraints thereby bringing the motor into compliance with requirements [17]. Unfortunately, more than 30 full scale RS Maverick motor tests were required to deduce the necessary "heterogeneity variables," i. e., although enlightened empiricism works, it is usually expensive.

*The author is interested in Fig. 2 propellants because their "coral structures" could protect regression rate determining processes from the core flow, i. e., propellants that resist erosive burning (and velocity coupling?).

The above demonstrates that present-time CFD predictions with ballistic-characterization BCs approach to low risk, cost effective solid rocket motor development is not robust. This begs the question: "How could solid rocketry age of development [1, 2] have achieved so much with 1D models and the same ballistic characterization information?" The answer is instructive.

(d) Since 1D models are compatible with ballistic characterizations deterministic information, impacts of their crudeness were ameliorated*.

(e) The past time plurality of important motor developments, in an environment where risk was necessary and tolerated in that sense, enabled empirical engineering and its concurrent hands-on training in the workplace.

The latter overcame information deficit on ballistic characterization with *additional*, *unstructured information*, e.g., motor failures, planned experiments' structured empiricism [17], etc. — that, over time, provided workplaces with facilities and experienced personnel with hands-on capabilities that could *achieve* low risk, cost effective motor developments *in this environment*. Therefore, although present time science-based approach has greater potential, it must have $\rho_{s,c}(\vec{x}_s, t)$, $r_s(\vec{x}_s, t)$, etc. and BS topography BC information to function robustly because information processing is ruled by "garbage-in equals garbage-out" no matter how hi-tech the information processing.

Present time has created DNS simulations of heterogeneous propellant deflagration, etc. [20]. Figure 3 presents an instantaneous tomogram of the temperature field† for heterogeneous propellant shown in Fig. 1 whereas Fig. 4 presents time histories of temperature for *ideal* microthermocouple in this field. These Rocfire Code simulations of heterogeneous propellant deflagration, etc. visualize nondeterministic aspects and enable quantitative assessments of deflagration phenomena *for their virtual environments*. On the one hand, Rocfire Code does not yet mimic BS melts, intuminescent binders, acceleration augmented burning (suggesting it is a BS melt phenomena), etc. On the other hand, Massa *et al.* [21] demonstrate rigorous spatial averaging requires the condensed-phase homogeneous, 1D energy equation has the form

$$\frac{\partial T}{\partial t} + r_b \frac{\partial T}{\partial x} = \alpha \frac{\partial^2 T}{\partial x^2} + \frac{S(x)}{\rho c} \tag{5}$$

and the heterogeneity source term $S(x)$ can be significant. Therefore, Rocfire Code *virtual reality* can stimulate the creation of and mentor the development

*Deur and Hessler [18] extend axial mode acoustic stability theory to include combustion noise and vortex phenomena, and Hessler and Glick [19] show that omni-present pressure oscillations can help estimate modal frequencies and stability margins in applications

†The corresponding gas speed tomogram presents panel contours of similar geometry.

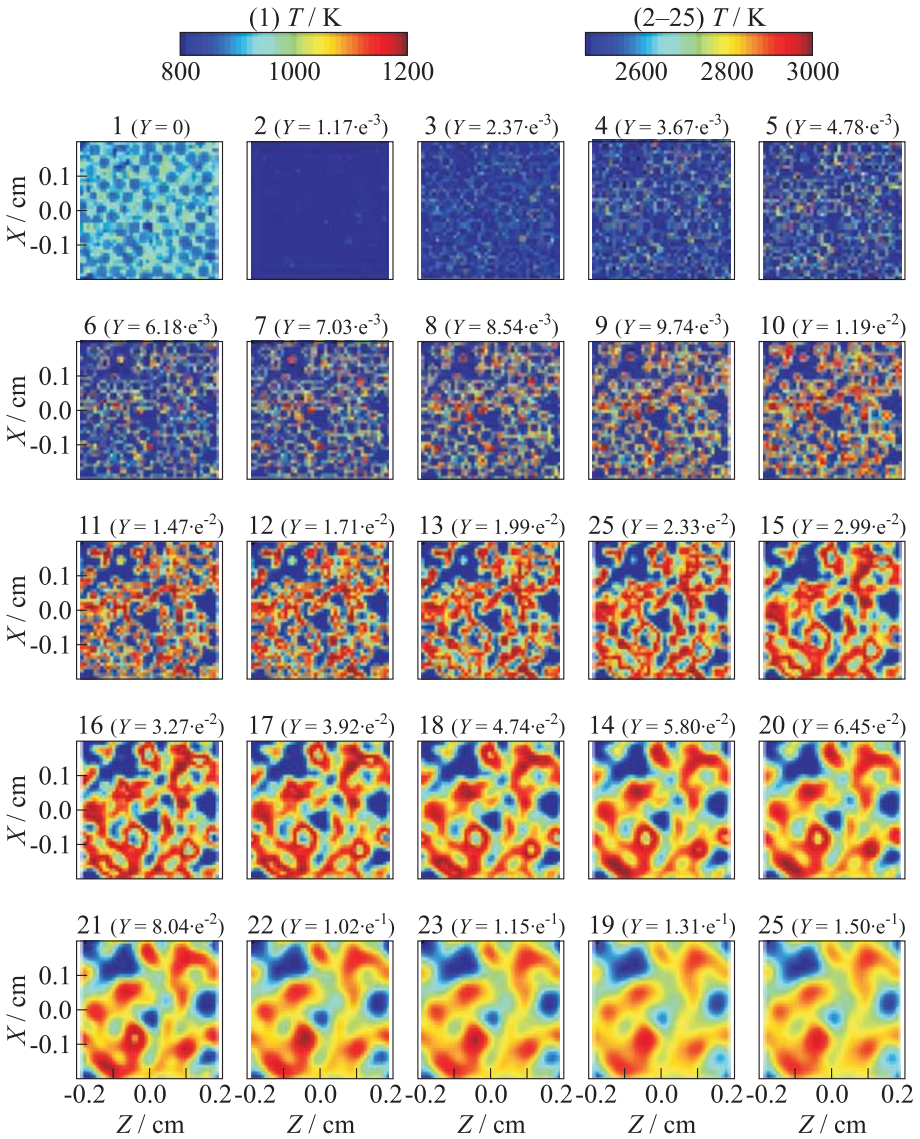

Figure 3 Temperature field $T(x, z, y_i, t = \text{fixed})$: HT/AP propellant (Rocfire Code courtesy T. L. Jackson). (Refer Glick, p. 42.)

of approximate models with dramatically reduced computational requirements* (note the analogy of this DNS mentoring to graduate education).

For idealized homogeneous propellant deflagrating in a quiescent, isobaric environment, each panel of Fig. 3 would have a uniform temperature and that temperature would increase monotonically from panel to panel with y_i, $i = 1, \ldots,$ 25, as altitude above the BS increased. Moreover, all of Fig. 4 time histories of temperature would be monotonically increasing with altitude and congruent when their initial displacements were accounted for. Therefore, Figs. 3 and 4 complexities demonstrate that heterogeneous-propellant nondeterministic morphology can significantly impact BS BCs and near-BS phenomena, e. g., Fig. 3 [3] snapshot Schlieren images. Figures 3 and 4 demonstrate equilibrium, typically assumed to occur by approximately 30-micron altitude [27], can be incomplete at 1500 μm, i. e., almost two orders of magnitude beyond expectations†. This is informed (and supported) by Povinelli [11] CN spectra, Korobeinichev [29] microthermocouple measurements (compare Fig. 12 in [29] with Fig. 4), and Fig. 3 [3] Schlieren images (the strand is ~ 3 mm wide).

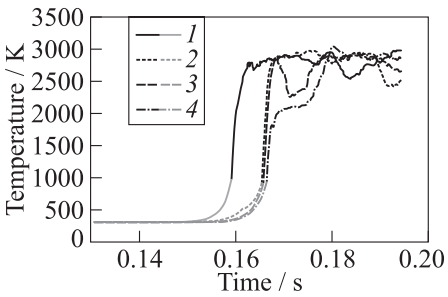

Figure 4 Ideal microthermocouple histories: HTPB/AP propellant (Rocfire Code simulation courtesy T. L. Jackson)

If the disjoint elements above are integrated, i. e., combine the past-time successful empiricism based on simple 1D models and ballistic characterizations augmented with real motor and supplementary experimental information with present-time computational and instrumentation capabilities, a strategy for progress emerges:

– improve ballistic characterization at the strand level with cine digital imaging and acoustic energy measures;

– enhance motor testing with omni-present pressure oscillation information and ultrasound diagnostic information;

*Over 40 years of BDP model developments [22–26] have failed to accomplish this critical step because naive averaging is part of the model's DNA.

†Ideal microthermocouple measurements of Fig. 3 differ significantly from idealized homogeneous-propellant monotonic expectation and exhibit large variations among identical microthermocouples in the same propellant and environment. It appears, Kubota [28] first connected these "impossible for idealized homogeneous propellant measurements" with heterogeneity.

– employ Rocfire Code based DNS to mentor model and hardware development; and

– continue the development of Rocfire Code genre.

Moreover, although the *virtual reality* of the Rocfire Code genre can deviate from reality, its *completely detailed* quantitative description at suboxidizer particle scales enables Popperian falsifications impossible in reality — a critical advantage.

The objective of this work is to sketch how this can be accomplished.

2 CRITICAL LITERATURE

The phenomenological viewpoint of section 1 demonstrates the critical importance of explicit, nondeterministic ballistic characterization information. Critical open literature is now examined to assess its information.

Price's [30] seminal criticism of idealized homogeneous propellant burning rate models argues

(f) they cannot robustly mimic heterogeneous-propellant local, spatiotemporal variations of regression rate, composition, temperature, topography, etc. across the BS at the oxidizer particle microscale (see [3, 11, 28, 29, 31, 32] artifacts); and

(g) spatial mean BS composition changes during transients [33, 34, 35, 36] (Steinz and Selzer's BS AP depletions during rapid depressurization extinguishments are compelling evidence) and

the experimental data support Price. Moreover, these experimental Schlieren images [3], CN spectra [11], microthermocouple [28, 29, 31], and line reversal pyrometer [32] measurements support Figs. 3 and 4 isobaric deflagration characteristics. In addition, optical temperature and/or specie measurements during and extinguished surface composition measurements after rapid depressurization extinguishments demonstrate that significant BS composition and flame temperature variations can occur during transients. Furthermore, Stokes *et al.* [37] rapid extinguishments demonstrate that erosive burning can alter composite-propellant BS topography inferring erosive burning alters impacts of items (f) and (g).

Logical consequences of items (f) and (g) are significant.

(h) Since quasi-steady (QS) processes are a sequence of steady-state processes, where BS composition is constrained to the virgin-propellant steady-state BS composition, they cannot robustly mimic item (g). Therefore, conventional QS and QSHOD transient burning rate models [38] are not robust for heterogeneous propellants.

(i) Schoyer's [39] analysis of L^* instability and item (g) [40] infer that conventional L^* models [41] are not robust. Consequently, Culick's [42] demonstration that conventional acoustic stability theory includes only conventional L^* models infers that conventional acoustic stability theory [43] is not robust for heterogeneous propellants.

George and Davidson [44] demonstrate that asymptotic turbulent flows are sensitive to their source spatiotemporal characteristics (large-eddy structures appear to propagate this information). Therefore, heterogeneous propellants $\vec{u}_{s,g}(\vec{x},t)$, $T_{s,g}(\vec{x},t)$, $\mathcal{M}_{s,g}(\vec{x},t)$, and BS topography information is expected to impact the flow field as RS Maverick's [17] development demonstrates (see also Figs. 2–4 and Figs. 3 and 4 in [3]).

Massa *et al.* [21] prove that robustly homogenized heterogeneous propellant requires heterogeneity related source terms $S(x,t)$ in the condensed-phase homogeneous 1D (HOD) energy equation, e. g., Eq. (5). Moreover, *Rocfire* Code results demonstrate that $S(x,t)$ can be significant. In addition, if Massa *et al.* BS smoothing function is applied to the flow field equations, e. g., Eq. (1), heterogeneity related source terms also appear there.

Therefore, idealized homogeneous-propellant smooth and uniform composition BS, and deterministic BCs, e. g., burning rate, acoustic admittance, etc., *require the items* (f) *and* (g) *heterogeneity information lost to be appropriately embedded in the condensed-phase and the flow field governing equations* if predictions for heterogeneous propellant grained applications are to be robust and provide deep understanding of the phenomena. Because the philosophical principle "*the whole is equal to or greater than the sum of its parts*" infers that information removed from one part (BCs) of the whole must be restored to another (field equations), it supports the generality of [21] mathematical results.

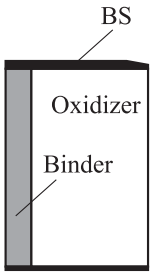

Figure 5 Sideways sandwich model

The QS reactive region of [21] Rocburn Code reveals it cannot robustly mimic nonsteady heterogeneous propellant deflagration effects of item (g). Therefore, on the one hand, Rocburn Code joins the BDP genre [22–26] of QS burning rate models whose (unmissed) absence of explicit items (f) and (g) information renders them impotent for robust flow field BCs. On the other hand, Schusser *et al.* [25] and Rasmusson and Frederick [26] combination of the Cohen and Strand model [24] QS reactive region with Fig. 5 sideways sandwich (homogeneous binder and oxidizer slabs) condensed-phase geometry enables item (g) predictions — a significant development ([45] provides a linearized version of [25]). Unfortunately, the sandwich homogeneous slabs preclude BS AP depletions observed in Steinz and Selzer's [34] rapid depressurization experiments. Therefore, these heterogeneous propellant models instan-

taneous mass burning rate and flame temperature predictions cannot be robust for either linear or nonlinear processes.

The literature above demonstrates intellectual thought and experimental dating from the late 1960s, 1970s, and recent analyses support the inferences of section 1 based on boundary value problem fundamentals, physical evidence, and rational thought.

3 REGENERATION

Sections 1 and 2 demonstrate that the absence of explicit, nondeterministic information from ballistic characterizations and naively homogenized burning-rate models prohibits low-cost performance predictions for heterogeneous propellant grained motors that are robust and provide deep understanding of the phenomena. The absence of explicit perspectives to these challenges in pertinent peer and editor reviewed journals* (see previous citations, e. g., [13]), texts [46, 47], monographs [48, 49], and the AIAA PAA series [3, 50–52] supports the hypothesis that the idealized homogeneous propellant is a Kuhnian paradigm [53] for Academy and scholarly publications: heterogeneity cannot be avoided in the workplace. Therefore, formal solid rocket education and research (particularly, graduate student research) are typically not robust for heterogeneous propellants and workplaces are intellectually separated from the Academy. Moreover, "hands-on" capability in the workplace is diminishing as retirement and/or death reduce their population of adept personnel and the scarcity of new developments and risk intolerance inhibits "hands-on" learning. Furthermore, because heterogeneous-propellant unique phenomenological and numerical challenges remain largely unrecognized, education and/or research that neither address these challenges nor put them in perspective produce disinformation and graduates taught to believe it.

This dismal description is probably excessive because intelligent people in competitive environments save *their best for themselves*, i. e., they do not freely share with competitors.

The objective of this section is to sketch a path out of the dismal situation and toward an internal ballistics that routinely treats heterogeneous propellant grained applications realistically within cost and risk constraints. Its focus is smaller hardware for six reasons:

1. Adequate ballistic characterization is the fundamental technical challenge.
2. Computational costs for CSAR type DNS are not prohibitive.

* *Web of Science* citation searches on [3, 11, 21, 28, 31–36] were graciously performed by Purdue University's Engineering Library. Results infer these seminal references are rarely cited and, when cited, the intent is seldom critical. Although this does not include journals from outside the USA, it suggests the spirit of present time in the USA.

3. Small propellant requirements enable engagement in the motor development process at the *beginning* of its propellant development effort: more information earlier enables better decisions sooner.

4. Although large motor developments are scarce, small motor developments are not.

5. Small motor developments are typically based on trial and error empiricism (Dr. J. N. Lilley, personal comment, 2006):

   (a) ballistic predictions are often more difficult (it is rare to find a large motor with 10 kpsi peak pressure and 50 ms burn time; erosive burning increases with decreasing motor size; etc.);

   (b) trial and error development has demonstrated superior robustness and cost effectiveness; and

   (c) because ballistic information obtained from small motor developments is relatively small, data increases from investments in improved instrumentation/testing should be large.

6. This focus enables a synergistic merging of the strengths of past and present time within the latter's constraints.

Because a plentiful, cost effective supply of real motor information is necessary, utilizing item 5 is *critical* to success.

3.1 Workplace Diagnostics

3.1.1 Optical strand burners

Idealized homogeneous-propellant ballistic-characterization determinism infers that artifacts of items (f) and (g) are insignificant. Therefore, on the one hand, early assessment of this presumption adequacy is crucial:

– if the candidate propellant behaves like idealized homogeneous propellant, the internal ballistics of the idealized homogeneous propellant should be adequate.

On the other hand, if the candidate fails this test, sufficient information to enable a heterogeneous-propellant internal-ballistics design is necessary. Therefore, because ballistic characterization begins with strands, routine strand burner characterization must provide sufficient information to make this decision.

Commercial availability of high-resolution, high-framing-rate digital image recorders enable concurrent burning rate and dispersed agglomerate quantification and qualitative assessment of deflagration phenomena at the strand level

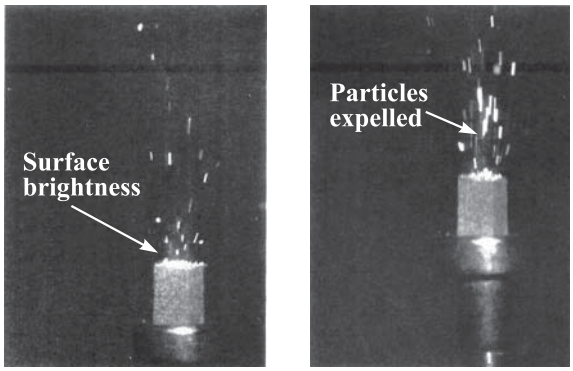

Figure 6 Vibration correlated Al dispersion at 1 atm, $\widehat{g} \sim 150g$; right: acceleration dispersion; left: acceleration retention [5] (courtesy A. Bandera and F. Maggi, Politecnico di Milano)

with conventional strand burner cost effectiveness and through put (strands burned/day). Moreover, because data and images are digital, computer technology enables automated data reduction, archival, and retrieval, i. e., a personnel independent, searchable, institutional memory.

Available technology can enhance an optical strand burner information. Pulse illumination can ameliorate image blur and overwhelm self-illumination. Moreover, Schlieren images provide density gradient information, e. g., Fig. 3 [3]. Multiple images can be recorded simultaneously with a split frame providing instantaneous comparisons. Time sequenced self- and externally illuminated images provide additional information.

Figure 2 demonstrates that optical strand burner tests can provide quantitative time-mean burning rate and qualitative deflagration process information concurrently. Moreover, Bandera *et al.* [54] demonstrate that quantitative metal agglomerate information can also be obtained. Therefore, for DC acceleration environments that do not retain the metal additive on the BS, quantitative measures of time-mean burning rate and metal additive agglomeration and qualitative measures of deflagration processes are in hand.

Figure 6 demonstrates that propellant deflagration in a window burner (in this case, the strand sting is vibrated) to characterize propellant deflagration is a vibrating environment. Because the sequence of cine digital images can be phase correlated with the vibrational environment, a sequence of images at identical vibrational states can be obtained and treated with the technology of [54] to characterize the time-mean burning rate and metal additive agglomeration characteristics. Therefore, the ensemble of this information would provide its phase dependence. Consequently, the technology of [54] can be employed to

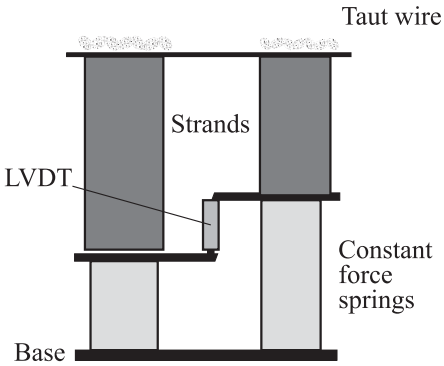

Figure 7 Schematic of taut wire difference measurement

concurrently characterize the time-mean burning rate and metal agglomeration quantitatively and deflagration process qualitatively in DC and AC acceleration fields.

Because strand deflagrations are audible, strand burner characterization should be possible. Moreover, this measurement could be addressed with Rocfire Code based simulations to optimize burner surface geometry, acoustic admittance, and multiple microphones. Moreover, because the integrand terms in the left hand side of Eq. (4) and the microphone signals would both be known, their relation could be optimized. In any event, systematic characterization at strand and small motor level could be employed to assess the ability of strand burner characterizations to predict omni-present pressure oscillations in applications.

The primary focus of strand burner characterization is to define propellants sensitivity to environment (pressure, initial temperature) and formulation variables. Therefore, because direct measurements of burning rate differences can reduce the uncertainty of differences estimated from two independent measurements by roughly 40%, direct measurements of burning rate differences in strand burners would be very valuable.

Taut wire BS positioning (Tim Parr, personal conversation, 2003) offers this measure along with reduced focal volume requirements and enhanced resolution for visual information recording (Fig. 7). It would apply for initial temperature and formulation sensitivities. Moreover, it doubles the information/burn. In addition, an optical fiber as taut wire offers concurrent BS temperature measurements. Moreover, another in the gas phase slightly displaced from and crossed with the BS offers correlogram based heterogeneity information, e. g., gas temperature and speed and distribution.

The above demonstrates that optical strand burners + digital image recorders + additional diagnostics enable more information/unit cost *routinely* for basic

formulation studies in academy and workplace environments. Although the initial investment is significant, operational expenses appear similar to conventional Crawford burners that provide only mass-mean burning rate information.

3.1.2 Rotating valve burners

Glick [55] demonstrated that concurrent correlation of $\overline{r}_b$ and $\mathcal{R}_p$ data with a phenomenological burning rate model can enhance information production and provide a calibrated phenomenological model. Moreover, because the flame temperature response function $\Theta_f = (\widehat{T}_f/\overline{T}_f)/(\widehat{p}/\overline{p})$ identifies when BS composition changes are significant during transients extending this approach to include concurrent $\overline{r}_b(\overline{p}, T_0)$, $\mathcal{R}_p(\omega_c\colon \overline{p}, T_0)$, and $\Theta_f(\omega_c\colon \overline{p}, T_0)$ information enhances their potential. There are two major challenges:

(1) concurrent $\overline{r}_b$, $\mathcal{R}_p$, and $\Theta_{f,p}$ measurements at fixed $\overline{p}$ and T_0 at a multiplicity of ω_c per burn with small propellant samples; and

(2) development of heterogeneous propellant deflagration models that can robustly predict these parameters.

The rotating valve burner [56] is attractive for the characterization function: its propellant grain is small and easily obtained from ice cream carton samples; existing hardware offer concurrent $\overline{r}_b$ and $\mathcal{R}_p$ measures; operational ultrasound diagnostics offer additional diagnostic information; and alternative rotating valve designs appear more robust.

The rotating-valve burner oscillatory-pressure environment is currently employed to estimate a propellant pressure-coupled acoustic admittance function by exploiting the burner large residence time τ_{ch} characteristics [56]. However, because pressure-coupled mass and flame temperature response functions are the propellant properties, assuming the rotating-valve area perturbations are invariant, i. e., every rotation is identical, enables concurrent mass and flame temperature response function estimates from measurements at two different residence time states τ_{ch1} and τ_{ch2} as

$$\Theta_f = \frac{\omega_c[(2\varepsilon_1 - 2\varepsilon_2)\tau_{\mathrm{ch2}} + \tau_{\mathrm{ch1}}(2\varepsilon_1 - 2\varepsilon_2)] + 2i\left(\omega_c^2\tau_{\mathrm{ch1}}\tau_{\mathrm{ch2}} - 1\right)(\varepsilon_1 - \varepsilon_2)}{\omega_c[\varepsilon_1\varepsilon_2(\tau_{\mathrm{ch1}} - \tau_{\mathrm{ch2}})]}\,\Psi + \frac{\gamma + 2i\omega_c(\tau_{\mathrm{ch1}} + \tau_{\mathrm{ch2}}) - 2\tau_{\mathrm{ch1}}\tau_{\mathrm{ch2}}\omega_c^2 + 1}{\gamma}; \quad (6)$$

$$R = \frac{\omega_c[(\varepsilon_1 - 2\varepsilon_2)\tau_{\mathrm{ch2}} - \tau_{\mathrm{ch1}}(\varepsilon_2 - 2\varepsilon_1)] + i\left(2\omega_c^2\tau_{\mathrm{ch1}}\tau_{\mathrm{ch2}} - 1\right)(\varepsilon_1 - \varepsilon_2)}{\omega_c[\varepsilon_1\varepsilon_2(\tau_{\mathrm{ch1}} - \tau_{\mathrm{ch2}})]}\,\Psi - \frac{1 + 2i\omega_c(\tau_{\mathrm{ch1}} + \tau_{\mathrm{ch2}}) - 4\omega_c^2\tau_{\mathrm{ch1}}\tau_{\mathrm{ch2}} - \gamma}{2\gamma}. \quad (7)$$

Therefore, *in principle*, a rotating-valve burner with a multifrequency rotating valve could estimate $\overline{r}_b(\overline{p}, T_0)$, $\mathcal{R}_p(\omega_c\colon \overline{p}, T_0)$, and $\Theta_f(\omega_c\colon \overline{p}, T_0)$ concurrently for its $\overline{p}$ and T_0 environment and formulation in a single test from pressure measurements and burner geometry alone. However, with ultrasound instrumentation direct, instantaneous burning rate (albeit potentially corrupted) and pressure-coupled mass response function information (potentially not robust) would be available *in real time*. Consequently, since burning rate and pressure-coupled mass response functions are the propellant properties, their ultrasound measures must be sensibly constant when mean pressure and variable throat area forcing are. Hence, ultrasound instrumentation provides indirect measures of the rotating-valve forcing function invariance that could be employed to assess the quality of characterizations based on Eqs. (6) and (7) and/or to control rotating valve parameters to maximize uniformity.

If the rotating valve is well designed, its stimuli are limited to its characteristic frequencies. Therefore, $p'(\omega_c)$ information in these "open intervals" of the spectrum offers direct combustion noise information. Moreover, because disparities between ultrasound and Eqs. (6) and (7) $\mathcal{R}_p(\omega_c\colon \overline{p}, T_0)$, measures depend on $r_s(\vec{x}, t)$, $T_{s,g}(\vec{x}, t)$, $\mathcal{M}_{s,g}(\vec{x}, t)$, etc. and BS topography, this approach also offers explicit heterogeneity related information.

Schusser *et al.* [45] linear transient burning rate mode upgraded with Eq. (5) offers a viable $\mathcal{R}_p(\omega_c\colon \overline{p}, T_0)$, $\Theta_f(\omega_c\colon \overline{p}, T_0)$, capable model in closed form *with* $S(x)$ *unknowns*. Therefore, concurrent correlation approach [55], extended to include Θ_f information, offers implicit estimates of $S(x)$ functions and a model that predicts $\overline{r}_b$, $\mathcal{R}_p$, and Θ_f for the characterized propellant.

Unfortunately, Schusser *et al.* model [45] cannot provide nondeterministic BS efflux information. Figure 8 sketches the life of an oxidizer particle from its entrance into the condensed-phase preheated regime (gestation), arrival at the BS (birth), and either burn-up on or dispersion from the BS (death). Beckstead [57] estimated that the regression rate and oxidizer/fuel ratio could vary during the AP particle life on the BS by roughly a factor of three. Therefore, since all of Fig. 8 states coexist on the BS, individual oxidizer particle responses with identical birth characteristics but different birth times can differ significantly. Indeed, if there is an ignition delay, a part of the BS AP is not burning. Moreover, for pressure oscillations with 1/frequency $\gg$ the oxidizer particle lifetime, the AP particle life is too short to see significant variations. However, when 1/frequency $\leq$ particle lifetime, pressure oscillations impact its life. Therefore, embedding this model in a statistical framework would embed Beckstead's oxidizer model in a propellant model.

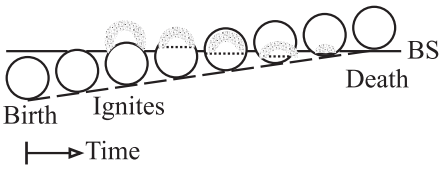

Figure 8 Diagram of oxidizer particle evolution

In the past, the veracity of [56] bulk mode analysis of the rotating valve burner was assumed. However, a *Rocfire* Code based DNS would provide a *virtual* assessment of similar, simplified rotating-valve burner models and details of their operation. Moreover, a virtual assessment of proposed ultrasound burning-rate measurement sensitivity to items (a) and (b) effects should be possible and would indirectly relate $\mathcal{R}_p(\omega_c\colon \overline{p}, T_0)$ measures from Eqs. (6) abd (7) and ultrasound information. Therefore, a number of indirect sources of items (f) and (g) information exist whose viability detailed simulation could assess (and optimize if viable).

Micci [58] demonstrated an MHD burner based on a uniform magnetic field and two-electrode MHD flowmeter for direct pressure-coupled acoustic admittance measurements. A characteristic of this burner is its extremely noisy MHD flow meter measurements. Moreover, because the MHD flowmeter measurement assumes that the flow field is axisymmetric but item (f) invalidates this assumption, this noise is expected and related to items (f) and (g). Therefore, estimates of items (f) and (g) attributes *in statistical form* may be possible. Since multiple electrodes and a uniform magnetic field enable velocity profile estimates in an axisymmetric flow, velocity profile measurements in asymmetric flows present a fundamental challenge. However, because the magnetic field is a free variable, are multiple electrodes and an appropriately nonuniform magnetic field that rotates adequate? In short, can multiple electrodes and a magnetic field that rotates during the measurements provide asymmetric velocity profile estimates in *a statistical sense*?

– A *Rocfire* Code based simulation could assess feasibility and, if viable, optimize apparatus parameters *virtually.*

3.1.3 Motor testing

Instrumentation for a conventional static motor test typically consists of thrust and head-end pressure measures. Hessler and Glick [19] demonstrate that modal frequency, modal stability margin, and flow structure estimates can be obtained from head-end pressure measurements if the omni-present pressure oscillation measurement has adequate s/n^*. Therefore, motor omni-present pressure oscillations provide a passive, nonintrusive, and essentially free information source. Moreover, Hedge and Strahle [60] demonstrate that omni-present pressure oscillations of the head-end are rich in acoustic information while those at the aft end are rich in fluid dynamic information. Consequently, extending the Hessler's approach to include both measures (and in between information from hoop strain

*Culick and Seywert [59] demonstrate that pulsing is more accurate. However, because this work employed neither optimal fittings, examined why identical basic information could produce different results for alternative but complimentary interrogations, nor contrasted the cost effectiveness and perils of pulse testing with Hessler's passive approach.

measures?) offers additional passive, nonintrusive and inexpensive information. In effect, the motor is instructing the listener aurally *in its language*: the challenge is to translate this into your language.

Champolin's translation of Egyptian hieroglyphics was a linguistic triumph; its key was the Rosetta Stone's message in a known language and hieroglyphics. Although this aid is denied ("solid rocket motor" is not spoken much less written), the present time has Rocfire Code based DNS that can correlate motor pressure oscillation information with BC, flow field, etc. information in quantitative detail to suboxidizer particle scales. Moreover, this is supplemented with qualitative measures of $\overline{r}_b(\overline{p}, T_0)$, $\mathcal{R}_p(\omega_c \colon \overline{p}, T_0)$, $\Theta_f(\omega_c \colon \overline{p}, T_0)$, metal agglomeration, and deflagration process acoustic energy emissions and qualitative deflagration process information (see, e. g., Fig. 2). Therefore, Rocfire Code based DNS ability to falsify hypotheses in its virtual reality offers indirect capability of estimating sufficient BC information from extended ballistic characterization and motor data. Indeed, the process is similar to (but different than) the past time successful application of inadequate ballistic characterization information, 1D models, and additional motor development and experimental information to successfully develop solid rocket motors.

A major challenge is the prohibitive computational expense of Rocfire Code based DNS for larger motors. Therefore, a computationally fast mimic appears necessary. How is this to be accomplished?

- CFD solutions of fundamental field equations with adequate BC information?
- CFD solutions of fundamental field equations with deterministic BCs and necessary nondeterministic BC information embedded in the field equations?
- An alternative approach?

The only certainty is that naive homogenizations (see, e. g., [61]) cannot achieve robust results and deep understanding of the phenomena.

3.2 Summary

Windowed strand burners with cine digital imaging and combustion noise diagnostics offer concurrent burning rate, dispersed agglomerate sizing, and visual and aural deflagration process characterizations at conventional stand burner cost/strand and time/strand. Moreover, information/unit cost can be enhanced with technical development, e. g., taut wire BS positioning and direct measurements of burning rate difference. Rotating valve burners can provide concurrent pressure-coupled mass and flame temperature response function estimates and

the MHD burner may have potential for statistical BS efflux characterizations. High s/n measurements of omni-present pressure oscillations at head and aft ends of motors during motor testing offer estimates of acoustic mode frequencies, stability margins, and flow field related information. Coupling this information with appropriate detailed simulations offers indirect characterization of items (a) and (b) effects necessary for robust application predictions. Since the exact path to this goal is not yet clear (and no single path may be sufficient), continuing development of detailed simulation, diagnostics, synergistic combinations, and effort are necessary.

4 CONCLUDING REMARKS

Internal ballistics predictions based on deterministic ballistic characterizations with necessarily homogeneous-propellant idealization are not robust for heterogeneous-propellant grained motors that dominate applications. Moreover, this idealization development/application without perspective to either heterogeneous propellant dominance or its innate challenges has inhibited research, corrupted education, and penalized development. Although ameliorated in the past time by necessity, empiricism, and increased risk tolerance, these detriments are exacerbated in this ages low risk and cost environment because explicit characterizations of nondeterministic BCs is now necessary for CFD based performance predictions that are robust.

Fortunately, improved ballistic characterizations can distinguish applications where deterministic models are adequate thereby enabling robust predictions for these specific applications. Moreover, improved ballistic characterization and motor testing provides explicit nondetermininistic information related to nondeterministic BC information necessary for robust predictions and deep understanding of phenomena in heterogeneous-propellant grained applications. In addition, Rocfire Code based DNS can mentor the development of technology to transform this explicit nondeterministic information into BC information that enables robust performance predictions because these DNS permit Popperian hypothesis falsifications. Because the path is uncertain, creative developments are necessary. The first step is to recognize heterogeneous propellants innate challenges; and the second step is to access small motor development information.

REFERENCES

1. Caveny, L. H., R. L. Geisler, R. A. Ellis, and T. L. Moore. 2003. Solid rocket enabling technologies and milestones in the United States. *J. Propul. Power* 19(6):1038–66.

2. Davenas, A. 2004. The development of modern solid propellants. *J. Propul. Power* 19(6):1108–28.
3. Summerfield, M., G. S. Sutherland, M. J. Webb, H. J. Taback, and K. P. Hall. 1960. Burning mechanism of ammonium perchlorate propellants. In: *Solid propellant rocket research*. Ed. M. Summerfield. ARS Progress in astronautics and rocketry ser. New York: Academic Press. 1:141–82.
4. Gallier, S., and F. Hiermard. 2008. Microstructure of composite propellants using simulated packings and X-ray tomography. *J. Propul. Power* 24(1):154–57.
5. Bandera, A. 2004. Aluminized solid propellant combustion under vibratory conditions. M.Sc. Thesis. Aerospace Engineering, Dipartimento di Energetica. Politecnico di Milano.
6. Guery, J. F., I-S. Chang, T. Shimada, M. Glick, D. Boury, E. Robert, J. Napior, R. Wardle, C. Perut, M. Calabro, R. Glick, H. Habu, N. Sekino, G. Vigier, and B. d'Andrea. 2008. Solid propulsion for space applications: An updated roadmap. IAC-08-C4.6.2.
7. Klager, K., and G. A. Zimmerman. 1992. Steady burning rate and affecting factors: Experimental results. In: *Nonsteady burning and combustion stability of solid propellants*. Eds. L. DeLuca, E. W. Price, and M. Summerfield. Progress in astronautics and aeronatutics ser. Washington, DC: AIAA. 143:Ch. 3.
8. Strand, L. D., and R. S. Brown. 1992. Laboratory test methods for combustion-stability properties of solid propellants. In: *Nonsteady burning and combustion stability of solid propellants*. Eds. L. DeLuca, E. W. Price, and M. Summerfield. Progress in astronautics and aeronatutics ser. Washington, DC: AIAA. 143:689–718.
9. Fry, R. S., *et al.* 2002. Evaluation of methods for solid propellant burning rate measurements. NATO. RTO Meeting Proceedings 91. AVT-089. Paper 34.
10. Ma, Y., W. K. Van Moorhem, and R. W. Shorthill. 2001. Experimental investigation of velocity coupling in combustion instability. *J. Propul. Power* 7(5):692–99.
11. Povinelli, L. A. 1965. A study of composite solid-propellant flame structure using a spectral radiation shadowgraph technique. *AIAA J.* 3(9):1593–98.
12. King, M. K. 1993. Erosive burning of solid propellants. *J. Propul. Power* 9(6):785–05.
13. Fischbach, S. R., J. Majdalani, and G. A. Flandro. 2007. Acoustic instability of the slab motor. *J. Propul. Power* 20(10):146–57.
14. Van Moorhem, W. K. 1982. Flow turning in solid-propellant rocket combustion stability analyses. *AIAA J.* 20(10):1420–25.
15. Kubota, N. 1981. Combustion mechanisms of nitramine composite propellants. *18th Symposium (International) on Combustion Proceedings*. The Combustion Institute. 187–94.
16. DeLuca, L.T., L. Galfetti, G. Colombo, F. Maggi, A. Bandera, V. A. Babuk, and V. P. Sinditskii. Microstructure effects in aluminized solid rocket propellants.
17. Ware, R. P. 1977. Reduced smoke Maverick rocket motor — verification program (U). Phase I: Final Report. RPL-TR-76-83.

18. Deur, J. M., and R. O. Hessler. 1984. Forced oscillation theory. AIAA Paper No. 84-1356.
19. Hessler, R. O., and R. L. Glick. 1998. Application of maximum entropy method to passively extract motor stability information. *Workshop on Measurement of Thermophysical and Ballistic Properties of Energetic Materials*. Politecnico di Milano. Milano, Italy.
20. Jackson, T. L. 2009. Overview of heterogeneous solid-propellant combustion. EUCASS Paper 324.
21. Massa, L. T. L. Jackson, and J. Buckmaster. 2004. Using heterogeneous propellant burning simulations as subgrid components of rocket simulations. *AIAA J.* 42(9):1889–900.
22. Cohen, N. S. 1980. Review of composite propellant burn rate modeling. *AIAA J.* 19(7):277–93.
23. Cohen, N. S. 1981. Response function theories that account for size distribution effects — a review. *AIAA J.* 19(7):907–12.
24. Cohen, N. S., and L. D. Strand. 1982. An improved model for the combustion of ammonium perchlorate composite propellants. *AIAA J.* 20(12):1739–46.
25. Schusser, M., F. E. C. Culick, and N. S. Cohen. 2002. Combustion response of ammonium perchlorate composite propellants. *J. Propul. Power* 18(5):1093–100.
26. Rasmussen, B., and R. A. Frederick. 2002. Nonlinear heterogeneous model of solid propellant combustion. *J. Propul. Power* 18(5):1986–92.
27. Friedman, R. 1967. Experimental techniques for solid-propellant combustion research. *AIAA J.* 5(7):1217–23.
28. Kubota, N. 1992. Flame structure of modern solid propellants In: *Nonsteady burning and combustion stability of solid propellants*. Eds. L. DeLuca, E. W. Price, and M. Summerfield. Progress in astronautics and aeronatutics ser. Washington, DC: AIAA. 143:Ch. 7; 233–59.
29. Korobeinichev, O. P. 2000. Flame structure of solid propellants. In: *Solid propellant chemistry, combustion, and motor interior ballistics*. Eds. V. Yang, T. Brill, and W. Ren. Progress in astronautics and aeronautics ser. Washington, DC. 185:Ch. 2.3; 335–54.
30. Price, E. W. 1969. Relevance of analytical models for perturbation of combustion of solid propellant. *AIAA J.* 7(1):153–54.
31. Sabadell, A. J., J. Wenograd, and M. Summerfield. 1965. Measurement of temperature profiles through solid-propellant flames using fine thermocouples. *AIAA J.* 3(9):1580–158.
32. Derr, R. L., and J. R. Osborn. 1970. Composite propellant combustion. *AIAA J.* 8(8):1488–91.
33. Krier, H., M. Summerfield, H. B. Mathes, and E. W. Price. 1969. Entropy waves produced in oscillatory combustion of solid propellants. *AIAA J.* 7(11):2079–86.
34. Steinz, J. A., and H. Selzer. 1971. Depressurization extinguishment of composite solid propellants: Flame structure, surface kinetics, and restart capability. *Combust. Sci. Technol.* 3:25–36.

35. Eisel, J. L., N. W. Ryan, and A. D. Baer. 1972. Combustion of NH_4ClO_4–polyurethane propellants: Pressure, temperature, and gas-phase composition fluctuations. *AIAA J.* 10(12):1655–61.
36. Schoyer, H. F. R., and R. T. M. de Bont. 1986. Experimental verification of temperature oscillations during combustion instability. *AIAA J.* 24(2):340-41.
37. Stokes, B. B., R. O. Hessler, and L. H. Caveny. 1976. Erosive burning of nonmetalized composite propellants — data acquisition and analysis. *13th JANNAF Combustion Meeting Proceedings* II:437.
38. DeLuca, L., E. W. Price, and M. Summerfield 1992. Nonsteady burning and combustion stability of solid propellants. In: *Nonsteady burning and combustion stability of solid propellants*. Eds. L. DeLuca, E. W. Price, and M. Summerfield. Progress in astronautics and aeronatutics ser. Washington, DC: AIAA. 143:Chs. 2, 14, 15.
39. Schoyer, H. F. R. 1983. Incomplete combustion: A possible cause of combustion instability. *AIAA J.* 21(8):1119–26.
40. Glick, R. L., and D. R. Mathes. 2007. L^* instability: Heterogeneous propellants. AIAA Paper No. 2007-5861.
41. Price, E. W. 1992. L^* instability. In: *Nonsteady burning and combustion stability of solid propellants*. Eds. L. DeLuca, E. W. Price, and M. Summerfield. Progress in astronautics and aeronatutics ser. Washington, DC: AIAA. 143:Ch. 9.
42. Culick, F. E. C. 1968. Some nonacoustic instabilities in rocket chambers are acoustic. *AIAA J.* 6(7):1421–23.
43. Culick F. E. C., and V. Yang. 1992. Prediction of the stability of unsteady motions in solid-propellant rocket motors. In: *Nonsteady burning and combustion stability of solid propellants*. Eds. L. DeLuca, E. W. Price, and M. Summerfield. Progress in astronautics and aeronatutics ser. Washington, DC: AIAA. 143:Ch. 18.
44. George, W. K., and L. Davidson. 2004. Role of initial conditions in establishing asymptotic flow behavior. *AIAA J.* 42(2):438–46.
45. Schusser, M., F. E. C. Culick, and N. S. Cohen. 2008. Analytical solution for pressure-coupled combustion response functions for composite solid propellants. *J. Propul. Power* 24(5):1058–67.
46. Davenas, A. 1993. *Solid rocket propulsion technology*. Oxford, England: Pergamon Press.
47. Sutton, G.P., and O. Biblarz. 2010. *Rocket propulsion elements*. 8th ed. New York: John Wiley and Sons.
48. Williams, F. A., M. Barrere, and N. C. Huang. 1969. *Fundamentals of solid propellant rockets*. Slough, England: AgardOGraph, Technivision Services.
49. Culick, F. E. C. 2002. Combustion instabilities in solid propellant rocket motors. Von Karman Institute. 2 lectures.
50. Kuo, K. K., and M. Summerfield, eds. 1984. *Fundamentals of solid propellant combustion*. Progress in astronautics and aeronatutics ser. New York: AIAA. 90.
51. DeLuca, L., E. W. Price, and M. Summerfield, eds. 1992. *Nonsteady burning and combustion stability of solid propellants*. Progress in astronautics and aeronatutics ser. Washington, DC: AIAA. 143.

52. Yang, V., T. B. Brill, and W.-Z. Ren, eds. 2000. *Solid propellant chemistry, combustion, and motor interior ballistics*. Progress in astronautics and aeronatutics ser. Washington, DC: AIAA. 184.

53. Kuhn, T. S. 1970. *The structure of scientific revolutions*. 2nd ed. Chicago: University of Chicago Press. Chs. V–VII.

54. Bandera, A., F. Maggi, L. T. DeLuca, V. Thoorens, J. F. Trubert, and O. Prusova. 2009. Size evaluation of solid rocket propellant agglomerates. EUCASS Paper 268.

55. Glick, R. L. 1999. Concurrent analysis of steady and nonsteady test data. AIAA Paper No. 1999-2803.

56. Brown, R. S., J. E. Erickson, and W. R. Babcock. 1974. Combustion response function measurements by the rotating valve method. *AIAA J.* 12(11):1502–10.

57. Beckstead, M. W. 1993. Solid propellant combustion mechanisms and flame structure. *Pure Appl. Chem.* 65(2):297–307.

58. Micci, M. M. 2008. Magnetic flowmeter burner measurements of a solid propellant pressure-coupled imaginary response. *J. Propul. Power* 24(1):149–50.

59. Culick, F. E. C., and C. Seywert. 1999. Some influences of noise on combustion instabilities and combustion dynamics. CPIA Pub. 691. 1:461–87.

60. Hegde, U.G., and W. C. Strahle. 1985. Sound generation by turbulence in simulated rocket motor cavities. *AIAA J.* 25(1):71–77.

61. McDonald, B. A., and S. Menon. 2005. Direct numerical simulation of solid propellant combustion in crossflow. *J. Propul. Power* 21(3):460–69.